High power-efficiency terahertz quantum cascade laser*

Yuan-Yuan Li(李媛媛), Jun-Qi Liu(刘俊岐)†, Feng-Qi Liu(刘峰奇)‡,
Jin-Chuan Zhang(张锦川), Shen-Qiang Zhai(翟慎强), Ning Zhuo(卓宁),
Li-Jun Wang(王利军), Shu-Man Liu(刘舒曼), and Zhan-Guo Wang(王占国)

Key Laboratory of Semiconductor Materials Science, Institute of Semiconductors, Chinese Academy of Sciences, and Beijing Key Laboratory of Low Dimensional Semiconductor Materials and Devices, Beijing 100083, *China*

(Received 24 February 2016; revised manuscript received 12 April 2016; published online 25 June 2016)

We demonstrate continuous-wave (CW) high power-efficiency terahertz quantum cascade laser based on semi-insulating surface-plasmon waveguide with epitaxial-side down (Epi-down) mounting process. The performance of the device is analyzed in detail. The laser emits at a frequency of ∼ 3.27 THz and has a maximum CW operating temperature of ∼ 70 K. The peak output powers are 177 mW in pulsed mode and 149 mW in CW mode at 10 K for 130-μm-wide Epi-down mounted lasers. The record wall-plug efficiencies in direct measurement are 2.26% and 2.05% in pulsed and CW mode, respectively.

Keywords: terahertz lasers, quantum cascade lasers, epitaxial-side down mounting

PACS: 42.55.Px, 73.63.Hs, 85.35.Be **DOI:** 10.1088/1674-1056/25/8/084206

1. Introduction

Terahertz quantum cascade laser (THz QCL) has become the most potential terahertz solid-state emitting source due to the characteristics of compactness, high efficiency and low consumption since its invention in 2002.[1] During the past years, THz QCLs have experienced great improvement in output power. In 2013, a peak pulsed output power of 470 mW per facet at 3.9 THz was obtained by stacking two symmetric active regions together via a direct wafer-bonding technique.[2] Recently, by designing the active region structure, an uncorrected peak output power of ∼ 1 W has been achieved in the broad area THz QCL at ∼ 3.4 THz based on semi-insulating surface-plasmon (SISP) waveguide.[3] Such values are high enough for most of the applications, for example, imaging through self-mixing technology.[4–6] In addition to high output power, high efficiency, and low consumption are also desirable for THz QCLs. In 2007, wall-plug efficiencies of 2.4% at 4 K in pulsed mode and 5.5% at 40 K in CW mode were assessed for 2.83-THz QCLs via an indirect method based on the analysis of the local lattice temperature as extracted by microprobe photoluminescence versus electrical power.[7] Actually, high efficiency THz QCL with high output power and low power consumption in CW operation is necessary for various applications, like astronomical spectroscopy, bio-medical applications, free-space communication and remote sensing.[8–11] Most of the high power THz QCLs are fabricated with SISP waveguide[1,12,13] due to the small confinement factor in the active region ($\Gamma \sim 0.1$–0.5). However, these lasers often exhibit large threshold current densities due to the same reason, thus a severe heat accumulation takes places in the active core. To improve the ability of SISP waveguide laser to dissipate heat, epitaxial-side down (Epi-down) mounting of THz QCL on sapphire submount was presented in 2013.[14] Additionally, Epi-down mounting technology has been widely adopted in mid-infrared quantum cascade laser due to its ability to remove heat substantially.[15,16] Therefore, SISP waveguide combined with Epi-down mounting technique is an ideal structure for realizing high power and high efficiency emission for THz QCL.

In this paper, we report high power-efficiency terahertz quantum cascade laser with SISP waveguide and Epi-down mounting process. The maximum slope efficiencies of 900 mW/A and 678 mW/A are obtained in pulsed and CW mode, respectively. The measured maximum output power is 149 mW in CW operation with a wall-plug efficiency of $> 2\%$.

2. Device design and fabrication

THz QCL wafer was grown by EPI GENII solid source molecular beam epitaxy (MBE) system on a semi-insulating GaAs substrate. The structure was composed of a bottom 0.5-μm highly-doped (Si, 2.5×10^{18} cm^{-3}) GaAs layer, active region and a top 0.1-μm highly-doped (Si, 5×10^{18} cm^{-3}) GaAs contact layer. The active core included 185 periods of $Al_{0.15}Ga_{0.85}As$/GaAs heterostructure with a layer sequence starting from the injector barrier of **54.6**/108/**18**/113/**37.8**/92.4/**41.5**/(105 + 76), where the layer thickness is in unit Å, AlGaAs barriers are in bold, and

*Project supported by the National Basic Research Program of China (Grant Nos. 2014CB339803 and 2013CB632801), the Special-funded Program on National Key Scientific Instruments and Equipment Development, China (Grant No. 2011YQ13001802-04), and the National Natural Science Foundation of China (Grant No. 61376051).

†Corresponding author. E-mail: jqliu@semi.ac.cn

‡Corresponding author. E-mail: fqliu@red.semi.ac.cn

© 2016 Chinese Physical Society and IOP Publishing Ltd

the Si-doped layer (3×10^{16} cm^{-3}) is underlined. An optimized doping profile was adopted to eliminate the influence of dopant migration. The 130-μm-wide light-emitting ridges were processed by optical lithography and wet chemical etching (H_3PO_4:H_2O_2:H_2O = 1:1:10) to the bottom highly-doped layer. Compared with Epi-up lasers, a supporting ridge was defined as being adjacent to the light-emitting ridge to facilitate another electrode for Epi-down mounting. After depositing a 450-nm-thick SiO_2 insulating layer, windows for metal evaporation were opened by wet etching. Two 15-μm-wide narrow stripes of Ge/Au/Ni/Au (26/54/15/150 nm) were deposited at the edges of each emitting ridge as well as on supporting ridges extending to the bottom highly-doped layer (separated by 55 μm from the emitting ridge) by lift-off technique. Thermal annealing for 15 s at 390 °C was followed to provide Ohmic contact under nitrogen atmosphere. Then Ti/Au layer was deposited, covering both of the emitting ridges and supporting ridges. An efficient SISP waveguide was formed by the covering metal on the emitting ridge and the bottom highly-doped layer. To further improve the ability to dissipate heat and facilitate wire bonding, a ∼ 6-μm gold layer was electroplated, covering the Ti/Au layer. After the substrate was thinned down to 150 μm, Ti/Au metal layer was deposited on the substrate side. In order to increase the output power and reduce the threshold current density, lasers with different cavity lengths were coated with an Al_2O_3/Ti/Au/Al_2O_3 high-reflectivity (HR) layer on the back facet. Finally, the device was mounted Epi-down on the patterned aluminum nitride (AlN) submount using indium solder. The AlN submounts were patterned with gold and indium to separate the emitting ridges and supporting ridges. Figure 1 shows the details of the device structure.

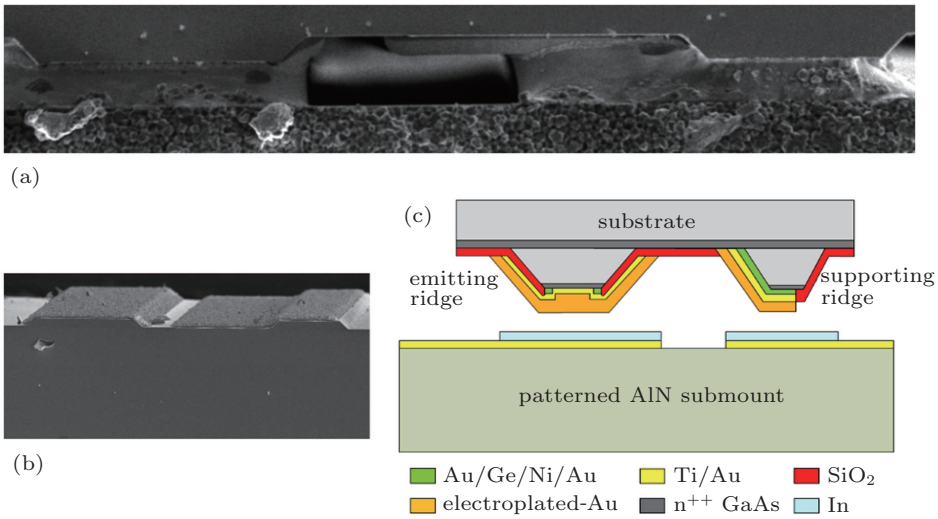


Fig. 1. (color online) (a) Scanning electron microscope (SEM) image of an Epi-down mounted device. (b) SEM image of a laser with Au-electroplated layer. (c) Cross section of the device with Epi-down mounting process.

3. Results and discussion

The devices are mounted on the cold finger of a liquid-helium cryostat equipped with a polyethylene (PE) window, of which the transmission is nearly 75% in THz range. An $f/2$ Winston cone with a diameter of 8.2 mm is placed in front of the laser facet to enhance collection efficiency. The single facet emitted power was measured by a broadband thermopile power meter and then corrected by a Thomas Keating (TK) absolute THz power meter. The measurement of spectrum is performed through a Fourier-transform infrared spectrometer (Bruker, Equinox55) with a resolution of 0.5 cm^{-1} in rapid scan mode. All pulsed measurements are taken at a 2-μs current pulse with a repetition rate of 5 kHz.

Pulsed peak output powers of 146 mW, 170 mW, and 177 mW are obtained from the 130-μm-wide Epi-down mounted devices at 10 K corresponding to the cavity lengths of 2, 2.5, and 3 mm, respectively. Figure 2 shows the typical light–current–voltage (*L*–*I*–*V*) curves of a 3-mm-long device at various heat-sink temperatures in pulsed mode. The measured peak output power is ∼ 177 mW with a threshold density of 190 A/cm^2 and a wall-plug efficiency of ∼ 1.98% at 10 K. At 77 K, the peak output power of ∼ 83 mW is still obtained with a wall-plug efficiency of 0.84%. The output power is high enough for various applications when the device is packaged in liquid nitrogen Dewar. The lasing is observed up to 100 K. The inset of Fig. 2 presents the empirical fitting of the threshold current density $J_{\rm th}$ dependence of the heat-sink temperature T. The characteristic temperature T_0 is extracted to be 30 K by the exponential function $J_{\rm th} = J_0 \exp(T/T_0)$.

Figure 3(a) displays the wall-plug efficiencies of 130-μm-wide Epi-down mounted devices in a temperature range from 10 K to 100 K in pulsed operation. The efficiency arrives at a maximum value of ∼ 2.26% at 10 K from a 2-mm-long device and decreases with heat-sink temperature and cavity length increasing. Figure 3(b) shows the slope efficiencies of the three devices the same as those in Fig. 3(a). The maximum slope

efficiency of ∼ 900 mW/A which is equivalent to a differential quantum efficiency of ∼ 65 photons per injected electron is also obtained from the 2-mm-long device. These slope efficiencies show the same trend as the wall-plug efficiencies, i.e., the shorter devices exhibit higher values at a certain temperature due to the higher mirror loss. Additionally, the efficiency difference between the devices decreases as the temperature increases, and at 100 K the wall-plug efficiencies of the three devices are nearly the same and their slope efficiencies are also approximately the same. This demonstrates the importance of temperature which has a great influence on the performance of THz QCLs.

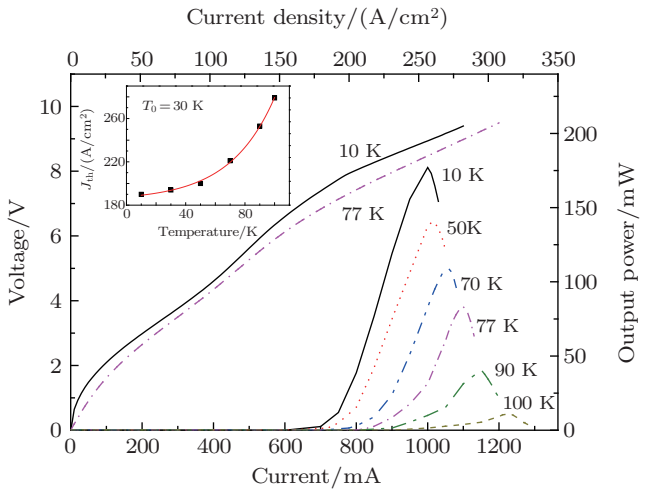


Fig. 2. (color online) Light–current–voltage (*L–I–V*) characteristics of a 130-μm-wide and 3-mm-long Epi-down mounted device working in pulsed mode at different heat-sink temperatures. The voltages of the device working at 10 K and 77 K are also presented. The inset shows the exponential fitting between the threshold current density and the temperature.

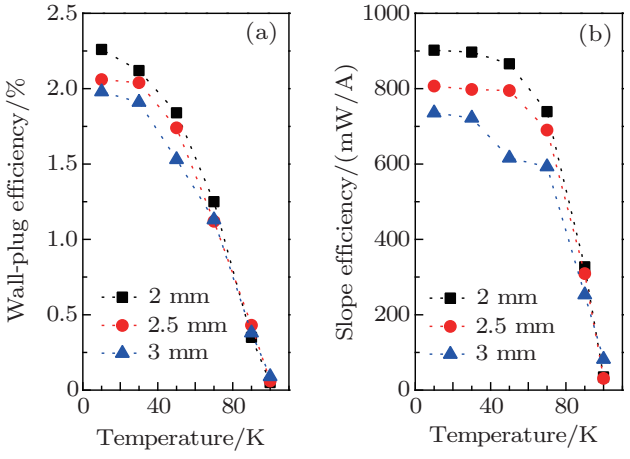


Fig. 3. (color online) (a) Plots of wall-plug efficiency versus temperature for 130-μm-wide Epi-down mounted devices with different cavity lengths. (b) Plots of slope efficiency versus temperature of the same devices at various temperatures.

The *L–I* characteristics of 130-μm-wide and 2-mm-long devices working in pulsed mode at various temperatures are shown in Fig. 4(a). Devices mounted epitaxial-up (Epi-up) and Epi-down are both presented. At a certain temperature, the peak output power of the Epi-down mounted device is slightly higher than that of the Epi-up one. Moreover, the two types of devices have the same maximum operating temperatures. It is clear that the Epi-down mounting process does not show a significant effect on the performances of devices due to the low heat accumulation in the active region in pulsed operation. Figure 4(b) shows the *L–I–V* characteristics of the same devices operated in CW mode. At 10 K, the peak output powers of the two types of devices are similar. The maximum power of ∼ 149 mW with a record wall-plug efficiency of ∼ 2.05% and a slope efficiency of 678 mW/A is obtained from the Epi-down mounted sample. With the increasing of temperature, the power difference between the two types of devices is gradually obvious. The maximum operating temperature of the Epi-down device is ∼ 70 K, which is almost 10 K higher than that of the Epi-up one. This illustrates that the Epi-down mounting process does improve the ability of THz QCL to dissipate heat in CW mode especially at high temperatures. The inset of Fig. 4(a) shows that the threshold current density of the Epi-down mounted device is always smaller than that of the Epi-up mounted device at a certain temperature in both pulsed and CW mode. The inset of Fig. 4(b) displays the emission spectrum for the Epi-down mounted device at a frequency of ∼ 3.27 THz at 10 K.

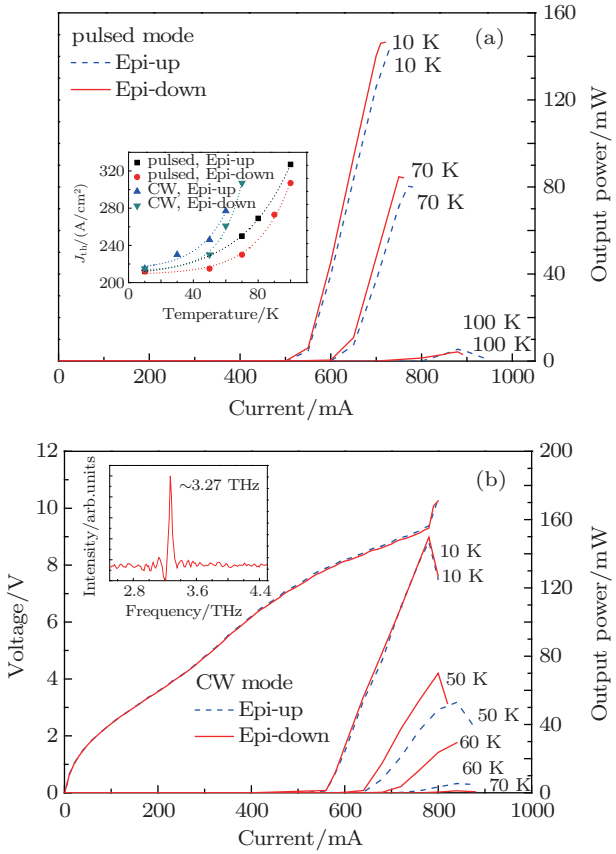


Fig. 4. (color online) (a) *L–I* characteristics of 130-μm-wide, 2-mm-long Epi-down and Epi-up mounted devices at various temperatures in pulsed mode. The inset displays the threshold current density versus temperature for devices in both pulsed and CW operation. (b) *L–I–V* characteristics of the same devices in CW mode. The inset shows the lasing spectrum for the Epi-down mounted device at 10 K.

In order to characterize the ability of the two types of devices to dissipate heat quantitatively, two-dimensional heat distribution is simulated based on a finite-element electromagnetic solver (COMSOL). The simulated results are shown in Fig. 5 when the devices are based on CW mode at peak current density $J_{\text{peak}} = 323$ A/cm^2 with the bottom of heat-sink at 60 K. The thermal conductivities are assumed to be $\kappa = 200$ W/m·K and 230 W/m·K for the highly-doped GaAs layer and semi-insulating GaAs substrate respectively,[17] and $\kappa = 50$ W/m·K is adopted for the active region.[18] The resulting maximum temperatures in the active region are 83 K and 72 K for Epi-up and Epi-down mounted devices, respectively, which indicates that the thermal transport property of the Epi-down mounted device is better. Such a discrepancy is evidence that Epi-down mounting structure improves the ability to remove the heat of the active region, and thus raises the maximum operating temperature in CW mode. The low value of the simulated $T_{\text{max,active}}$, compared with the measured $T_{\text{max,pulsed}}$ (100 K) in pulsed mode, may be caused by the poor heat removal effect of the bonding interface.

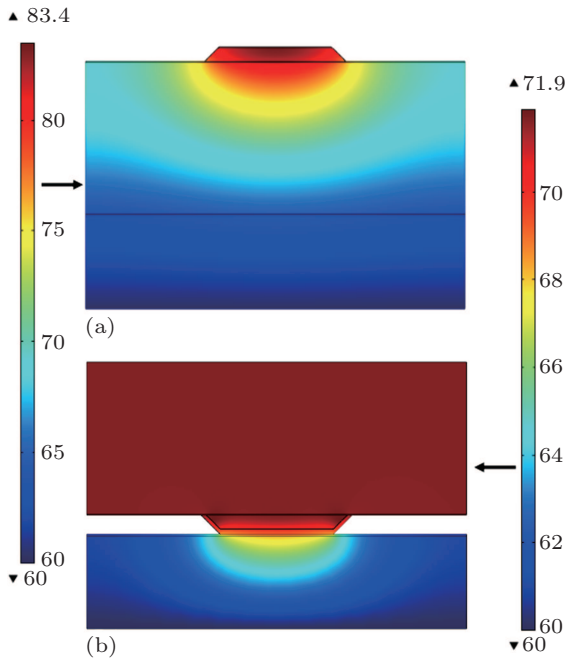


Fig. 5. (color online) Two-dimensional heat distributions in (a) Epi-up mounted device and (b) Epi-down mounted device, simulated with COMSOL. The temperature of the heat-sink is set to be 60 K.

4. Conclusions

In this work, we demonstrate high power-efficiency operation of Epi-down mounted THz QCLs. Optical output powers of ~ 177 mW with a threshold density of ~ 190 A/cm^2 at 10 K and ~ 83 mW at 77 K are obtained in pulsed mode respectively. CW emission at ~ 3.27 THz with an output power of ~ 149 mW is achieved at 10 K, and the maximum operating temperature is up to ~ 70 K. The record wall-plug efficiencies of 2.26% and 2.05% are realized in pulsed and CW mode, respectively. We believe that the development of Epi-down mounting technology will further improve the performances for THz QCLs.

Acknowledgment

The authors would like to thank Ping Liang and Ying Hu for their help in device fabrication processing.

References

[1] Köhler R, Tredicucci A, Beltram F, Beere H E, Linfield E H, Davies A G, Ritchie D A, Iotti R C and Rossi F 2002 *Nature* **417** 156
[2] Brandstetter M, Deutsch C, Krall M, Detz H, MacFarland D C, Zederbauer T, Andrews A M, Schrenk W, Strasser G and Unterrainer K 2013 *Appl. Phys. Lett.* **103** 171113
[3] Li L H, Chen L, Zhu J X, Freeman J, Dean P, Valavanis A, Davies A G and Linfield E H 2014 *Electron. Lett.* **50** 309
[4] Dean P, Lim Y L, Valavanis A, Kliese R, Nikolić M, Khanna S P, Lachab M, Indjin D, Ikonić Z, Harrison P, Rakić A D, Linfield E H and Davies A G 2011 *Opt. Lett.* **36** 2587
[5] Valavanis A, Dean P, Lim Y L, Alhathlool R, Nikolić M, Kliese R, Khanna S P, Indjin D, Wilson S J, Rakić A D, Linfield E H and Davies G 2013 *IEEE Sensors Journal* **13** 37
[6] Mezzapesa F P, Petruzzella M, Dabbicco M, Beere H E, Ritchie D A, Vitiello M S and Scamarcio G 2014 *IEEE Trans. Terahertz Sci. Technol.* **4** 631
[7] Vitiello M S, Scamarcio G, Spagnolo V, Dhillon S S and Sirtori C 2007 *Appl. Phys. Lett.* **90** 191115
[8] Hübers H W, Eichholz R, Pavlov S G and Richter H 2013 *J. Infrared Milli. Terahz. Waves* **34** 325
[9] Kim S M, Hatami F, Harris J S, Kurian A W, Ford J, King D, Scalari G, Giovannini M, Hoyler N, Faist J and Harris G 2006 *Appl. Phys. Lett.* **88** 153903
[10] Liu C W, Zhai S Q, Zhang J C, Zhou Y H, Jia Z W, Liu F Q and Wang Z G 2015 *J. Semicond.* **36** 094009
[11] Danylov A A, Goyette T M, Waldman J, Coulombe M J, Gatesman A J, Giles R H, Qian X F, Chandrayan N, Vangala S, Termkoa K, Goodhue W D and Nixon W E 2010 *Opt. Express* **18** 16264
[12] Rochat M, Ajili L, Willenberg H, Faist J, Beere H, Davies G, Linfield E and Ritchie D 2002 *Appl. Phys. Lett.* **81** 1381
[13] Ulrich J, Zobl R, Finger N, Unterrainer K, Strasser G and Gornik E 1999 *Physica B* **272** 216
[14] Krüger O, Kreutzmann S, Prasai D, Wienold M, Sharma R, Pittroff W, Weixelbaum L, John W, Biermann K, Schrottke L, Schnieder F, Erbert G, Grahn H T and Tränkle G 2013 *IEEE Photon. Technol. Lett.* **25** 1570
[15] Gmachl C, Sergent A M, Tredicucci A, Capasso F, Hutchinson A L, Sivco D L, Baillargeon J N, Chu S N G and Cho A Y 1999 *IEEE Photon. Technol. Lett.* **11** 1369
[16] Tsekoun A, Go R, Pushkarsky M, Razeghi M and Patel C K N 2006 *Proc. Natl. Acad. Sci.* **103** 4831
[17] Blakemore J S 1982 *J. Appl. Phys.* **53** R123
[18] Kumar S, Williams B S, Kohen S, Hu Q and Reno J L 2004 *Appl. Phys. Lett.* **84** 2494